DALTON
FULL PAPER

Metal complexes with a chiral N_4 symmetrical Schiff base. Crystal structures of the ligand and its Cu(II) and Ni(II) "mono-helicates" †

Miguel Vázquez,[a] Manuel R. Bermejo,*[a] Jesús Sanmartín,[a] Ana M. García-Deibe,[a] Carlos Lodeiro[b] and José Mahía[c]

[a] *Dpto. de Química Inorgánica, Facultade de Química, Universidade de Santiago de Compostela, Campus Sur, Santiago de Compostela, 15706, Spain*
[b] *Dpto de Química, C.Q.F.B. Facultade de Ciências e Tecnología, Universidade Nova de Lisboa, Monte de Caparica, 2825, Portugal*
[c] *Servicios Xerais de Apoio á Investigación, Universidade da Coruña, Campus da Zapateira s/n, A Coruña, 15071, Spain*

Received 6th August 2001, Accepted 14th December 2001
First published as an Advance Article on the web 20th February 2002

The N_4 Schiff base ligand *N,N′*-bis(2-tosylaminobenzylidene)-1,2-diaminocyclohexane (H_2cyTs) and its divalent metal (Fe, Co, Ni, Cu, Zn and Cd) complexes have been prepared. Of these compounds only Zn(*trans*-cyTs)·3H_2O can be considered as blue luminescent (λ = 435 nm, φ = 0, 12). Either demetallation or the absence of the tosyl groups, results in a loss of fluorescence. The X-ray crystal structures of a diastereoisomeric mixture of H_2cyTs and its (1*R*,2*R*)-enantiomer, as well as those corresponding to Cu(*trans*-cyTs)·MeCN and Ni(*trans*-cyTs)·MeCN have been solved. The Cu(II) and Ni(II) ions assume tetrahedrally distorted square planar coordination geometries, involving the four donor N-atoms of the dianionic ligand. The spatial disposition of both tosyl groups prevents global consideration as an usual symmetric helicand.

Introduction

Readily-prepared N_4 imine ligands, in which the spacer plays an important role in aspects such as control of directionality of ligand strands within a helix or its microarchitecture, have been reported.[1] In recent years, we have worked with $O_2N_2O_2$ and N_4 symmetrical molecular threads useful for obtaining self-assembled cage-like complexes[2] and bis-helicates.[3,4] In this context, we have designed a series of N_4 Schiff bases containing a two- or three-membered spacer, whose flexibility is conditioned by the chain length or the presence of an aromatic ring. The characterization of some of these Schiff bases derived from the condensation of 2-tosylaminobenzaldehyde with aliphatic[5a,5b] or aromatic[5c] diamines has been already described. The study of the photophysical properties of this type of ligands and their complexes has attracted our attention, since other compounds containing sulfonamido-substituted aromatic rings have been described as fluorescent.[6,7]

Recently, we have reported the syntheses and X-ray crystal structures of [4 + 4] nickel and zinc bis-helicates, as well as cobalt and copper mono-helicates,[4] containing a N_4 symmetrical molecular thread with a $(CH_2)_3$ spacer. Now, we are interested in the influence of the spacer on the formation of helicates, as well as on their fluorescence emission. We describe herein the synthesis, X-ray crystal structure and fluorescence emission studies of the ligand H_2cyTs [*N,N′*-bis(2-tosylaminobenzylidene)-1,2-diaminocyclohexane] and some of its derivatives (Scheme 1). Since this is a chiral molecule, some studies were performed on a diastereoisomeric mixture and/or its (1*R*,2*R*)-enantiomer. The X-ray crystal structures of tetrahedrally distorted square-planar Cu(*trans*-cyTs)·MeCN and Ni(*trans*-cyTs)·MeCN are also presented.

† Electronic supplementary information (ESI) available: some ^{13}C NMR data and UV-VIS spectra of Zn(*trans*-cyTs)·3H_2O + TFA. See http://www.rsc.org/suppdata/dt/b1/b107116p/

Results and discussion

Analytical data and mass spectroscopy

The found empirical formulae M(cyTs)·*x*H_2O (M = Fe, Co or Cu, *x* = 1–3), M(*trans*-cyTs)·*x*H_2O (M = Ni, Zn or Cd, *x* = 1–3) and Zn(*trans*-cy)(MeCN) suggest that the ligands are bis-deprotonated in the neutral metal(II) complexes. Bearing in mind the variety of stereoisomers that these complexes can present, their nomenclature only specifies a *cis*-*trans* notation when prepared from a pure ligand derivative.

The FAB mass spectra of all complexes containing $cyTs^{2-}$ show intense peaks related to the presence of $M^+ - x H_2O$ fragments. This points to a solvating nature rather than to a coordinating behaviour of the water molecules. However, the FAB mass spectrum of Zn(*trans*-cy)(MeCN) shows a peak related to the presence of a M^+ fragment at 423.2 (8%) that could indicate the coordination of an acetonitrile molecule to the Zn(II) ion. It must be noted that no peaks attributable to dimeric species are detected in the complex spectra.

IR spectroscopy

Most of the complexes show a shifting of 10–20 cm^{-1} to lower wavenumber values of ν(C=N) (1632 cm^{-1} in the free ligand spectrum). This suggests the coordination of $cyTs^{2-}$ through the imine nitrogen atoms. In contrast, a slight shifting to higher values was detected for the cobalt and copper complexes.

Other bands, attributable to ν(C–N), $\nu_{as}(SO_2)$ and $\nu_s(SO_2)$ modes, undergo substantial negative shifts for all complexes. This fact is in agreement with the amide N-atoms participating in coordination to the metal ion.[4]

NMR studies

The ^1H NMR spectra of (1*R*,2*R*)-H_2cyTs, (1*R*,2*R*)-H_2cy and their diamagnetic complexes were recorded in dmso-d_6 as

 DOI: 10.1039/b107116p

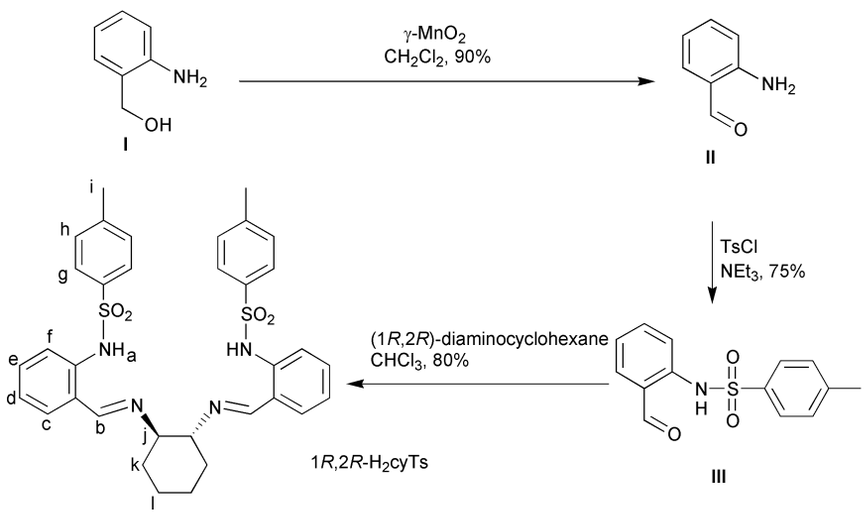

Scheme 1 Schematic representation of the synthetic procedure for (1*R*,2*R*)-H_2cyTs and the labelling scheme for the ^{1}H NMR studies.

solvent. Assignment of the signals was according to our experience[4,5] and to the available literature.[8–10]

The disappearance of the amide protons (H_a in Scheme 1) present in the free ligands is in agreement with the bis-deprotonation of the Schiff base. Those protons corresponding to the tosyl groups (H_g, H_h and H_i), as well as a doublet from the benzylidene ring (H_c), appear shifted in the range 0.3–0.6 ppm to lower field upon complexation. This shifting is higher for Zn(*trans*-cyTs)·3H_2O than for Ni(*trans*-cyTs)·MeCN·3H_2O. The remaining benzylidene ring protons are only very slightly shifted upfield. The imine protons (H_b) are not displaced after complexation, in contrast to the shift to lower field observed for the imine protons in a bis-helicate[4b] containing a very similar ligand, with a $(CH_2)_3$ spacer. Likewise, the cyclohexane ring protons appear unaffected by the coordination, as three groups of signals, centred at about 3.6, 1.9 and 1.6 ppm, appear where equatorial and axial protons can be anticipated.

UV-VIS absorption and fluorescence emission studies

The UV absorption spectrum of (1*R*,2*R*)-H_2cyTs, which was performed in dry acetonitrile solution, exhibits three bands (see Experimental section). Two of them were also observed for 2-tosylaminobenzaldehyde (**III**, in Scheme 1). Whereas Cd(II) complexation of (1*R*,2*R*)-H_2cyTs does not affect λ absorption in its UV spectrum, coordination to Zn(II) leads to a substantial shift to higher values. The only spectral feature that seems to indicate cadmium coordination is a very weak band at about 362 nm. This could be a sign of a different interaction between (1*R*,2*R*)-cyTs^{2-} and Cd(II). The relative stability of Zn(*trans*-cyTs)·3H_2O and Cd(*trans*-cyTs)·2H_2O in acidic acetonitrile solutions was studied by addition of trifluoroacetic acid, TFA (see ESI).† A demetallation reaction seems to occur after addition of about 20 equivalents of TFA for Zn(*trans*-cyTs)·3H_2O and about four equivalents for Cd(*trans*-cyTs)·2H_2O. This was deduced from the appearance of the same absorption spectrum as previously registered for the free ligand. Therefore, the zinc complex appears to show a higher stability towards acidity. Unfortunately, additional measurements to determine the ligand–Zn(II) interaction constant were unsuccessful.

Fluorescence emission studies in acetonitrile solutions show that 2-tosylaminobenzaldehyde **III** exhibits an intense luminescence at about 498 nm, whilst (1*R*,2*R*)-H_2cyTs, obtained from its condensation with (1*R*,2*R*)-diaminocyclohexane shows a residual luminescence under the same conditions. We have found that other aliphatic spacers, such as $(CH_2)_2$ or $(CH_2)_3$, do not prevent the fluorescence emission of their corresponding Schiff base ligands.[5] Thus, the active unit may be located on the 2-tosylaminobenzaldehyde residue, although the origin of the fluorescence is still unknown. Anyway, the spacer seems to play an important role in the fluorescence properties of this type of ligand.

The chelation of Zn(II) to cyTs^{2-} involves an enhancement of the fluorescence emission (CHEF effect, *i.e.* Chelation Enhancement of the Fluorescence), whereas the coordination of other metal ions such as Cd(II) affect it only very slightly. Zn(*trans*-cyTs)·3H_2O shows an intense luminescence at about 435 nm in acetonitrile solution, as its quantum yield (Φ = 0.12) indicates. Other evidence for the relation between luminescence and the presence of the tosylamino groups could be the non-emissivity, under the same conditions previously used, of Zn(*trans*-cy)(MeCN). This complex contains a ligand equivalent to (1*R*,2*R*)-H_2cyTs, but lacking tosyl groups.

The variation of the Zn(*trans*-cyTs)·3H_2O fluorescence emission with TFA can be observed in Fig. 1. The successive

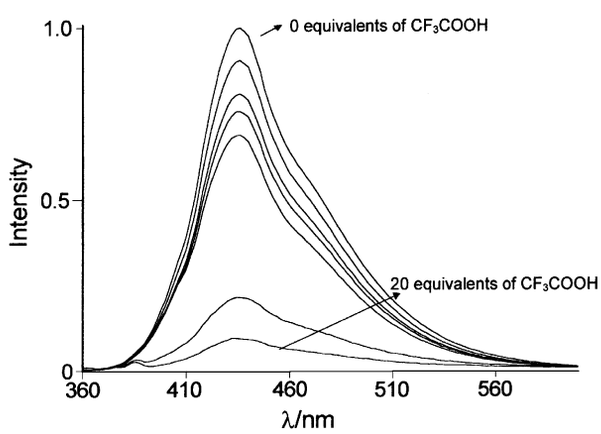

Fig. 1 Normalized fluorescence emission spectra (λ_{exc} = 314 nm) for Zn(*trans*-cyTs)·3H_2O in acetonitrile solution showing the effect of the number of TFA equivalents added (0, 0.5, 2, 4, 6, 14 and 20).

addition of acid leads to a progressive decrease of the fluorescence that finally (above 20 equivalents of TFA) results in a residual emission, characteristic of the free ligand. This is consistent with the demetallation hypothesis mentioned above, and points out the reversibility of the complexation reaction depending on the acidity of the medium.

Both UV-VIS data in the solid state (diffuse reflection, DR) and in DMF solution (see Experimental section) suggest square-planar environments for Ni(II) and Cu(II) ions in their corresponding complexes. However, these spectral data seem to indicate that the coordination geometry for Co(cyTs)·3H_2O and Fe(cyTs)·2H_2O could be described as pseudo-octahedral.

Table 1 Crystal and structure refinement data

	H_2cyTs	(1*R*,2*R*)-H_2cyTs·0.25H_2O	Ni(*trans*-cyTs)·MeCN	Cu(*trans*-cyTs)·MeCN
Empirical formula	$C_{34}H_{36}N_4O_4S_2$	$C_{34}H_{36.5}N_4O_{4.25}S_2$	$C_{36}H_{37}N_5NiO_4S_2$	$C_{36}H_{37}CuN_5O_4S_2$
M	628.79	633.29	726.54	731.37
Crystal system	Monoclinic	Monoclinic	Monoclinic	Monoclinic
Space group	$P2_1/c$	$P2_1$	$P2_1/c$	$P2_1/c$
a/Å	11.2798(3)	11.4723(2)	12.673(3)	12.6852(2)
b/Å	15.2754(4)	15.3201(3)	28.740(7)	28.7169(3)
c/Å	18.9152(3)	19.1700(3)	10.0593(16)	10.2814(2)
β/°	92.921(1)	93.286(1)	104.726(16)	106.6670(10)
U/Å^3	3254.92(13)	3363.72(10)	3543.5(13)	3587.96(10)
T/K	298(2)	298(2)	298(2)	293(2)
Z	4	4	4	4
μ(Mo-Kα)/mm^{-1}	0.207	0.201	0.711	0.770
No. reflections collected	13155	14383	14866	15058
No. independent reflections	5722	11278	6282	6325
R_{int}	0.0662	0.0193	0.0834	0.0309
Data/restraints/parameters	5722/0/454	11278/1/806	6282/0/435	6325/0/480
*R*1, *wR*2 [$I > 2\sigma(I)$]	0.0623, 0.1127	0.0517, 0.1052	0.0549, 0.1251	0.0510, 0.1316
*R*1, *wR*2 (all data)	0.1532, 0.1456	0.0792, 0.1223	0.1057, 0.1476	0.0771, 0.1456
Residuals/e Å^{-3}	0.164, −0.289	0.249, −0.186	0.445, −0.804	0.341, −0.435

Magnetic studies

Magnetic susceptibility measurements at room temperature for the iron, cobalt and copper compounds give magnetic moment values typical of magnetically diluted M(II) ions. Fe(cyTs)·$2H_2O$ presents a magnetic moment very close to that expected for a high-spin octahedral complex (5.2 μ_B). However, the magnetic moment of Co(cyTs)·$3H_2O$ (4.5 μ_B) is slightly lower than that attributed to octahedrally coordinated Co(II) ions (4.8–5.2 μ_B). Finally, the magnetic moment of Cu(cyTs)·H_2O (2.0 μ_B) is in accordance with a tetrahedrally distorted square-planar geometry, as its crystal structure confirms. Likewise, its ESR spectrum shows a line around the $g = 2$ region, coherent with an axial symmetry.

Single crystal X-ray diffraction studies

H_2cyTs and (1*R*,2*R*)-H_2cyTs·0.25H_2O. The crystal structure of H_2cyTs was solved as a mixture containing the *meso*, (1*R*,2*R*) and (1*S*,2*S*) diastereoisomers. Table 1 provides a summary of the crystal data, data collection and refinement parameters. The asymmetric unit contains the six carbon atoms of the 1,2-diaminocyclohexane residue disordered in two different positions. These correspond to the *trans* and *cis* isomers of the diamine residue, which coexist with 79.3% and 20.7% occupation sites, respectively. The *trans* molecules are responsible for the presence of the (1*R*,2*R*) isomer in the asymmetric unit, its (1*S*,2*S*) enantiomer being symmetry generated. The *cis* isomer, which is denoted by ' in the labelling scheme, yields the *meso* form. All the diastereoisomers show a chair conformation and Fig. 2 shows these three possibilities for the diamine residue. Some selected bond distances and angles are listed in Table 2 for the different molecules.

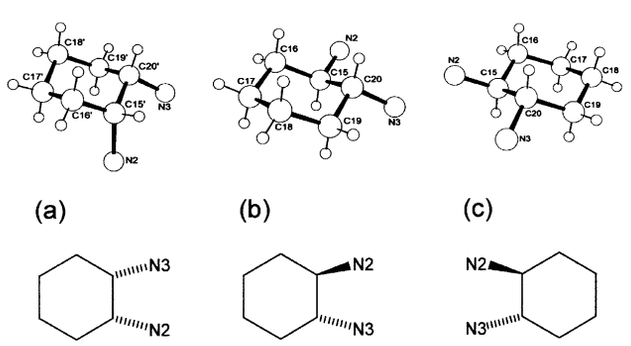

Fig. 2 Schematic and PLUTO-style representations of the 1,2-diaminocyclohexane residue for the three H_2cyTs diastereoisomers: (*a*) *meso*-H_2cyTs; (*b*) (1*R*,2*R*)-H_2cyTs and (*c*) (1*S*,2*S*)-H_2cyTs.

As a result of the complexity induced by the presence of an adiastereoisomeric mixture for some experiments, the pure (1*R*,2*R*)-H_2cyTs enantiomer was subsequently synthesized and its crystal structure was also determined. In this case, the asymmetric unit comprises two crystallographically distinct, but chemically equivalent ligand units, as well as a water molecule with a half occupation site. The two ligand units (denoted by "a" and "b" in the numbering scheme) are in a very similar conformation to that previously found for H_2cyTs. These three ligand units show many similarities, so that only one of them (that labelled with "a") has been represented in Fig. 3. Therefore, we will simultaneously discuss general

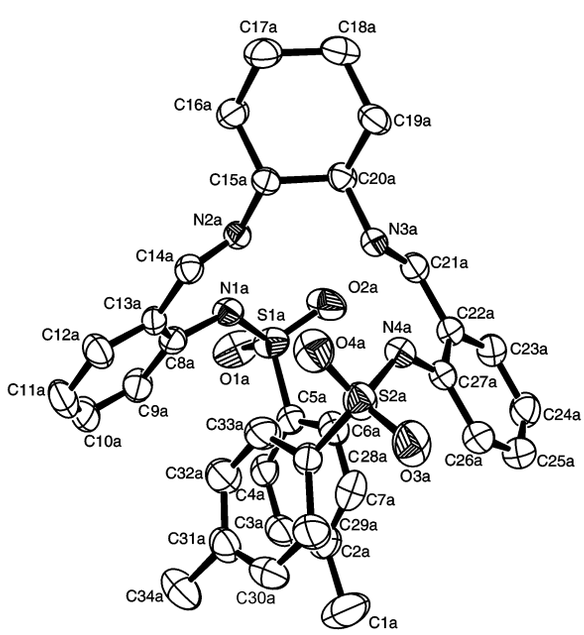

Fig. 3 ORTEP view (30% probability) of molecule "a", present in the asymmetric unit of (1*R*,2*R*)-H_2cyTs·0.25H_2O. Parentheses are omitted for clarity.

features of the molecular structures. Bond lengths and angles are within the range found in other very similar and previously characterized compounds[4,5,11] and do not merit further discussion.

The packing scheme and spatial molecular arrangement are controlled by weak interactions, in which the tosyl groups are involved. Thus, face to face π-stacking seems to exist between both terminal tosyl rings (Fig. 3), whose centers are *ca.* 4.1 Å apart. Likewise, edge to face interactions can be observed

Table 2 Selected distances (Å) and angles (°) for the ligands H_2cyTs and (1*R*,2*R*)-H_2cyTs·0.25H_2O

	H_2cyTs		(1*R*,2*R*)-H_2cyTs·0.25H_2O	
	(1*R*,2*R*), (1*S*,2*S*)	*meso* (′)	(a)	(b)
N(2)–C(14)	1.267(4)		1.262(4)	1.260(4)
N(2)–C(15)	1.405(8)	1.89(3)	1.465(4)	1.469(4)
N(3)–C(20)	1.482(9)	1.49(3)	1.469(4)	1.468(4)
N(3)–C(21)	1.266(4)		1.259(4)	1.264(4)
S(1)–N(1)	1.626(3)		1.628(3)	1.623(3)
S(1)–O(1)	1.440(3)		1.410(3)	1.421(3)
S(1)–O(2)	1.426(3)		1.444(3)	1.420(3)
S(2)–N(4)	1.629(3)		1.628(3)	1.637(3)
S(2)–O(3)	1.431(3)		1.425(3)	1.432(3)
S(2)–O(4)	1.436(3)		1.435(3)	1.431(3)
C(14)–N(2)–C(15)	118.4(5)	116.0(14)	117.2(3)	118.5(3)
C(20)–N(3)–C(21)	115.8(5)	130.5(13)	119.0(3)	118.8(3)
S(1)–N(1)–C(8)	128.8(3)		126.1(2)	127.7(2)
S(2)–N(4)–C(27)	127.5(3)		127.7(3)	127.6(3)
O(1)–S(1)–O(2)	120.8(2)		120.0(2)	120.8(2)
O(3)–S(2)–O(4)	120.35(18)		118.9(2)	119.7(2)
N(2)–C(15)–C(20)–N(3)	−62.1(7)	−51(3)	−60.2(3)	−62.1(4)
C(14)–N(2)–C(15)–C(20)	160.4(5)	162(2)	143.9(3)	149.7(3)
C(21)–N(3)–C(20)–C(15)	136.3(5)	140(2)	134.0(3)	138.0(3)
N(2) ··· N(3)	2.852(5)		2.866(4)	2.882(4)
N(1) ··· N(4)	5.346(5)		5.751(4)	5.786(4)
N(1) ··· N(2)	2.629(4)		2.669(4)	2.642(4)
N(3) ··· N(4)	2.634(4)		2.639(4)	2.632(4)
O(2) ··· O(1w)			2.995(15)	

between the tosyl and benzylidene rings, their centroids being at a distance of 4.9 Å. No intramolecular π-stacking interactions have been observed in related imines with other aliphatic spacers,[5a,5b] such as $(CH_2)_3$ or $(CH_2)_2$, where both tosyl groups were arranged in opposing positions in a pseudo-stepped conformation. In this case, the cyclic central spacer lacks flexibility and its subsequent inability to turn, leads the Schiff base to wrap around itself, which seems to form a sort of cavity (Fig. 4).

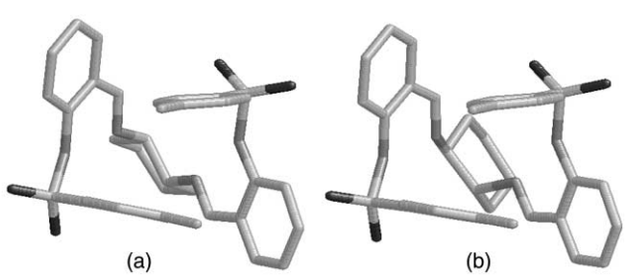

Fig. 4 Stick view of: (a) (1*R*,2*R*)-H_2cyTs and (b) *meso*-H_2cyTs, showing the N_4 cavity in the solid state packing. The atom positions have been selected from the crystal structure of the diastereoisomeric mixture of H_2cyTs.

This spatial arrangement of (1*R*,2*R*)-H_2cyTs (Fig. 4a) suggests that, with a simple torsion around the azomethine groups and the subsequent repulsion of the tosyl groups, this ligand could provide a single pseudo-planar N_4 compartment. Both (1*R*,2*R*) and (1*S*,2*S*) enantiomers, with their imine N-atoms in equatorial positions seem to favour a helical conformation and they are probably suitable for accommodating a metal centre in a pseudo-planar environment. However, the imine N-atoms are in both equatorial and axial positions in the *meso* diastereoisomer (Fig. 4b). Consequently, the flexibility required to coordinate a unique metal ion would need a high distortion of the cyclohexane ring, which may even promote a conformational change. This could lead the ligand to favour $N_2 + N_2$ chelation to two different metal centres, as found in the literature,[10] although in our case, the steric hindrance promoted by the terminal tosyl groups probably disfavours this arrangement.

Cu(*trans*-cyTs)·MeCN and Ni(*trans*-cyTs)·MeCN. Firstly, we must point out that a joint discussion was considered the most suitable, due to the structural similarities observed between these two complexes. Their crystal and refinement data are included in Table 1.

Slow evaporation at room temperature of saturated acetonitrile solutions of Cu(cyTs)·H_2O and Ni(*trans*-cyTs)·MeCN·3H_2O allow the isolation of crystals of Cu(*trans*-cyTs)·MeCN and Ni(*trans*-cyTs)·MeCN, respectively, suitable for single crystal X-ray diffraction studies. These have determined that their asymmetric units consist of discrete molecules of M(*trans*-cyTs) (M = Ni or Cu) and a solvated acetonitrile molecule. This is disordered in the case of Cu(*trans*-cyTs)·MeCN, since its terminal C-atom occupies two different sites (61.0 and 39.0%). The absence of hydrogen or π-stacking interactions leads to a weak packing scheme, which allows the presence of relatively significant vacant spaces, which are occupied by occluded solvent molecules.

The molecular structure of Ni(*trans*-cyTs)·MeCN is represented in Fig. 5, and the most significant bond distances and angles are included in Table 3. Despite preparing this complex with the pure (1*R*,2*R*)-H_2cyTs, and the asymmetric unit containing this form, the (1*S*,2*S*) derivative can be symmetry generated. This reveals that complexation implied a conformational change for 50% of the ligand molecules, at least in this case. This has lead to the fact that, although the complex was prepared with pure (1*R*,2*R*)-H_2cyTs, it had been denoted *trans*.

With regard to Cu(*trans*-cyTs)·MeCN, its 1,2-diaminocyclohexane residue shows four of its C-atoms on two different sites with calculated 52.7% and 47.3% occupation factors, corresponding to both (1*R*,2*R*) and (1*S*,2*S*) derivatives, respectively. No occurrence of the *cis* derivative was detected, so that this complex was also denoted *trans*. Those atoms corresponding to the (1*S*,2*S*) enantiomer derivative are denoted by ’ in the labelling scheme. Both derivatives are represented in Fig. 6a and 6b, with the atom labelling scheme used in Table 3, which lists the most relevant bond distances and angles.

The Ni–N bond distances are noteworthy since they are shorter than the average values found for other nickel complexes with N-donor ligands also containing tosyl groups.[4a,12]

Table 3 Selected bond distances and angles for Ni(*trans*-cyTs)·MeCN and Cu(*trans*-cyTs)·MeCN

Ni(*trans*-cyTs)·MeCN		Cu(*trans*-cyTs)·MeCN	
Ni(1)–N(1)	1.925(3)	Cu(1)–N(1)	1.960(3)
Ni(1)–N(2)	1.883(3)	Cu(1)–N(2)	1.963(3)
Ni(1)–N(3)	1.871(3)	Cu(1)–N(3)	1.952(3)
Ni(1)–N(4)	1.919(3)	Cu(1)–N(4)	1.966(3)
N(2)–C(14)	1.281(5)	N(2)–C(14)	1.282(5)
N(2)–C(15)	1.477(5)	N(2)–C(15)	1.542(10)
		N(2)–C(15′)	1.523(14)
N(3)–C(20)	1.476(5)	N(3)–C(20)	1.569(9)
		N(3)–C(20′)	1.524(12)
N(3)–C(21)	1.287(5)	N(3)–C(21)	1.273(5)
N(1)–S(1)	1.611(3)	N(1)–S(1)	1.593(3)
N(4)–S(2)	1.613(4)	N(4)–S(2)	1.597(3)
N(2)–Ni(1)–N(1)	91.13(14)	N(2)–Cu(1)–N(1)	88.67(13)
N(2)–Ni(1)–N(4)	167.53(15)	N(2)–Cu(1)–N(4)	157.72(16)
N(3)–Ni(1)–N(1)	167.88(15)	N(3)–Cu(1)–N(1)	158.16(15)
N(3)–Ni(1)–N(2)	85.84(14)	N(3)–Cu(1)–N(2)	83.74(13)
N(3)–Ni(1)–N(4)	89.83(14)	N(3)–Cu(1)–N(4)	90.66(13)
N(4)–Ni(1)–N(1)	95.42(15)	N(4)–Cu(1)–N(1)	103.57(13)
N(2)–C(15)–C(20)–N(3)	−41.0(4)	N(2)–C(15)–C(20)–N(3)	−54.4(10)
		N(2)–C(15′)–C(20′)–N(3)	63.5(16)
C(14)–N(2)–C(15)–C(20)	−142.4(4)	C(14)–N(2)–C(15)–C(20)	−144.7(7)
		C(14)–N(2)–C(15′)–C(20′)	153.7(10)
C(21)–N(3)–C(20)–C(15)	−138.4(4)	C(21)–N(3)–C(20)–C(15)	−151.7(7)
		C(21)–N(3)–C(20′)–C(15′)	145.9(10)
N(1) ··· N(2)	2.720	N(1) ··· N(2)	2.741
N(1) ··· N(4)	2.844	N(1) ··· N(4)	3.084
N(2) ··· N(3)	2.557	N(2) ··· N(3)	2.613
N(3) ··· N(4)	2.676	N(3) ··· N(4)	2.786

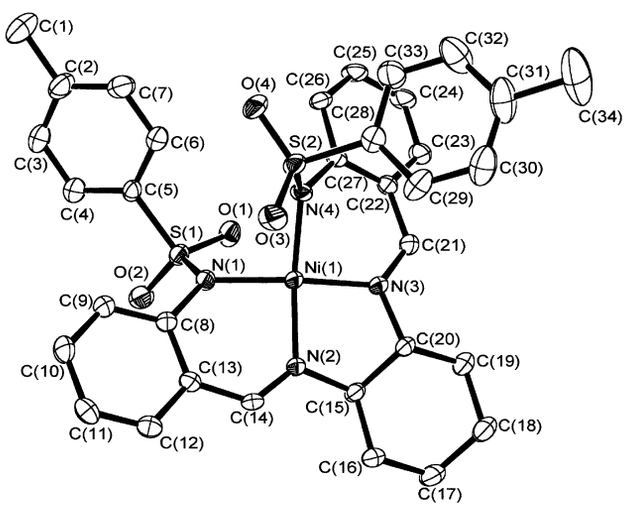

Fig. 5 ORTEP view of the *P* helicate present in the Ni(*trans*-cyTs)·MeCN crystal structure. Ellipsoids are drawn at 40% probability.

The Cu–N bond distances are also slightly shorter than those found for related complexes.[13,14] They are also slightly shorter than those corresponding to other copper complexes containing a related dianionic ligand with a three-methylene spacer.[4b] The steric hindrance promoted by the bulky tosyl groups, leads to long M ··· M distances that avoid any interaction between the metal centres.

Both Ni(II) and Cu(II) ions assume a tetrahedrally distorted square planar coordination geometry, involving the four N-atoms of the dianionic ligand. This tetrahedral distortion is rather pronounced for the Cu(II) chromophore, which is deduced from the values of the half-stepped distances displayed by a least-squares calculated plane [+0.3022(17), −0.3635(21), +0.3576(21), −0.2964(17) Å and −0.1743(16), +0.1948(18), −0.1980(18), +0.1774(16) Å for N(1), N(2), N(3) and N(4), in Cu(*trans*-cyTs)·MeCN and Ni(*trans*-cyTs)·MeCN, respectively]. The dihedral angle of only about 13.44(14)° (25.10(12)° for the Cu(II) complex) formed by the two opposite six-membered chelate rings also shows a less severe tetrahedral distortion for the Ni(II) complex.

The five-membered chelate ring formed by the *trans*-diaminecyclohexane residue and the metal ion in Ni(*trans*-cyTs)·MeCN, is the least planar ring, the farthest atoms from the plane appearing at about ±0.22 Å. This calculated plane forms dihedral angles of near 26.45(24)° and 32.50(20)° with the other two six-membered chelate rings (Fig. 7), which are slightly different to those formed by the (1*R*,2*R*) derivative in Cu(*trans*-cyTs) (*ca.* 27.4 and 18.17°). The N(2)C(15′)-C(20′)N(3) chelate ring corresponding to the (1*S*,2*S*) derivative of Cu(*trans*-cyTs)·MeCN is slightly less planar (maximum half-step distances about ±0.37 Å) than that found for the (1*R*,2*R*) derivative, with farthest atoms at about ±0.32 Å. However, this calculated plane forms rather smaller dihedral angles with the two opposite six-membered chelate rings (15.98(50)° and 9.52(82)°). These arrangements lead one to consider a helical conformation of the N_4 donor ligand, which is wrapping around the metal centres (Fig. 7). The different spatial disposition of both tosyl groups prevents global consideration as an usual symmetric helicand thread. Despite the smaller angles formed by the chelate rings in the case of the (1*S*,2*S*) derivative, the spacer is clearly protruding from the helix.

The metal ion size and its stereochemical preferences are crucial in microarchitecture selection. A sign of this influence could be provided by a similar ligand, but containing a $(CH_2)_3$ spacer, that gives rise to Co(II) and Cu(II) mono-helicates[4b] and to a nickel(II) bis-helicate.[4a] These results could have been induced by the effective ionic radii[15] of tetracoordinated Co^{2+} (72 pm), Cu^{2+} (71 pm) and Ni^{2+} (63–69 pm), and by a flexible spacer that allows a N_2 + N_2 binucleating behaviour. This is also an example of the significance of the spacer length and flexibility. In our present case, the short cyclic spacer and its inability to turn give reduced flexibility, which seems to prevent binucleating behaviour, and only mono-helicates could be obtained with $cyTs^{2-}$ containing the *trans* spacer derivatives. Although dinuclear complexes could be prepared with ligands

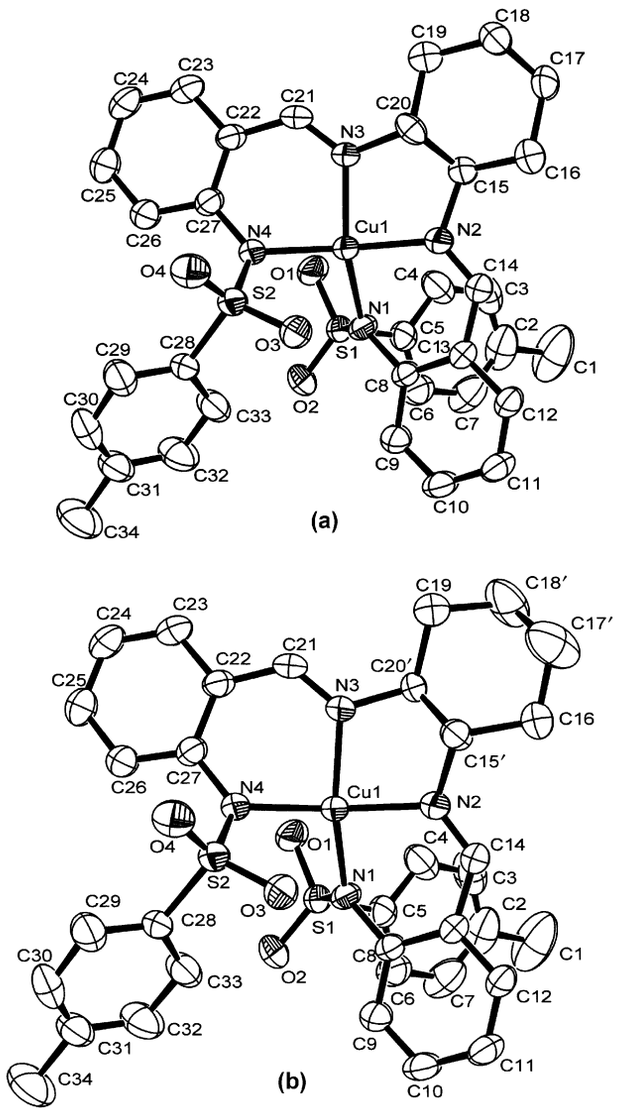

Fig. 6 ORTEP view of the two helicates simultaneously contained in the Cu(*trans*-cyTs)·MeCN asymmetric unit: (a) the (1*R*,2*R*)-*P* and (b) the (1*S*,2*S*)-*P*. The atom positions of the spacer have been selected from the disordered crystal structure of Cu(*trans*-cyTs)·MeCN. Ellipsoids are drawn at 40% probability and parentheses are omitted for clarity.

derived from the *cis* isomer of the spacer,[10] this does not happen in our Cu(II) complex.

Aspects related to helicity, such as wrapping angle, pitch or chirality, among others, could be discussed and compared with those corresponding to Cu(PTs)·1.5MeCN.[4b] Since both wrapping angle and pitch can significantly change their values depending on different considerations, such as the actual helix extremities or the helical axis declination, only qualitative aspects will be considered.

Neither Cu(*trans*-cyTs)·MeCN nor Ni(*trans*-cyTs)·MeCN, complete a twist around the metal centre if we only heed the donor atoms, so that both wrapping angles would be less than 360°. However, if we consider the whole ligand, the tosyl groups slightly exceed this value, as Fig. 7 shows. In that sense, we could indicate the S ··· S distances as being a close value to the pitch, being *ca*. 4.594 and 4.508 Å, for Cu(*trans*-cyTs)·MeCN and Ni(*trans*-cyTs)·MeCN, respectively. In both cases, the wrapping angles are significantly lower than that found for Cu(PTs)·1.5MeCN, which is probably related to a considerably higher chelate angle, induced by the $(CH_2)_3$ spacer [97.9(2)°]. Likewise, from the comparison of those angles formed by the different chelate planes corresponding to Cu(PTs)·1.5MeCN (Fig 7d), we can deduce a longer pitch. The short pitch could

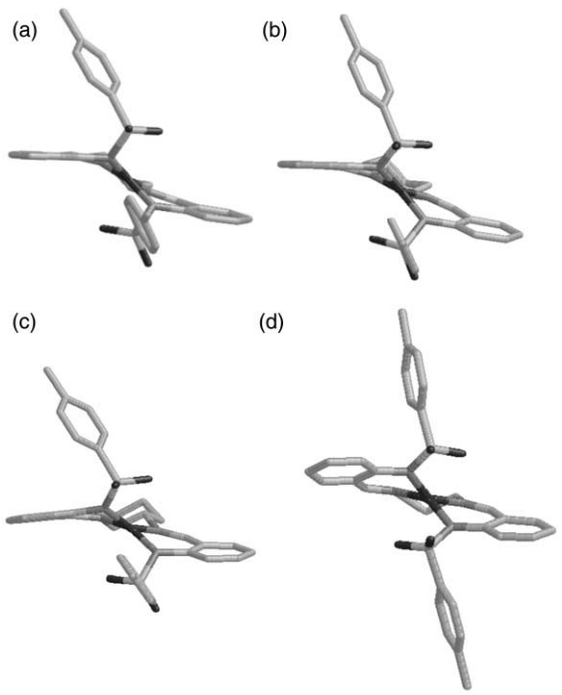

Fig. 7 Stick view of *P* helicates for: (a) Ni(1*R*,2*R*-cyTs), (b) Cu(1*R*,2*R*-cyTs), (c) Cu(1*S*,2*S*-cyTs) and (d) Cu(PTs).[4b] PTs^{2-} = *N*,*N*′-bis(2-tosylaminobenylidene)-1,3-diaminopropane.

cause the difference observed for the tosyl group conformations, since the shorter is the pitch the higher seems to be their steric hindrance.

With respect to the chirality, it is known that metal-assisted assembly of helicates gives a racemic mixture of *Plus* (*P*) and *Minus* (*M*) helices,[16,17] although several chiral ligands have been designed to achieve selective formation of *P* or *M* helicates.[18] In our case, this type of diastereoisomeric excess has not occurred. The asymmetric units of both metal complexes contain the *P* helices, but the *M* forms can be symmetry generated. Thus, we have obtained a racemic mixture of (1*R*,2*R*)-*P* and (1*S*,2*S*)-*M* helices for Ni(*trans*-cyTs)·MeCN.

When we used the described diastereoisomeric mixture of H_2cyts, *vide supra*, to interact with Cu(II) ions only the *trans* derivatives yielded Cu(II) complexes. In the asymmetric unit we can find both (1*R*,2*R*)- and (1*S*,2*S*)-*P* helices, which are symmetry-related to (1*S*,2*S*)-and (1*R*,2*R*)-*M* helices, respectively. This makes a total of four diastereoisomers for this compound. In this sense, we must point out that despite this no *P* or *M* diastereoisomeric excess can be detected for Cu(*trans*-cyTs), the majority (52.7%) of diastereoisomers are (1*R*,2*R*)-*P*, and (1*S*,2*S*)-*M*, which contain the chair-conformed spacer (Fig. 7) lying down on the helix.

Conclusion

The packing scheme and spatial molecular arrangement of the ligand crystal structures are controlled by π-stacking interactions, in which the tosyl groups are involved. Both (1*R*,2*R*) and (1*S*,2*S*) derivatives were found for Ni(II) and Cu(II) complexes, but no presence of the *meso* diastereoisomer was detected. Both Ni(II) and Cu(II) ions assume a tetrahedrally distorted square planar coordination geometry, involving the four N-atoms of the dianionic ligand. This tetrahedral distortion is rather pronounced for the Cu(II) chromophore. The N_4 donor ligand displays a helical conformation, where the different spatial arrangement of the tosyl groups prevents global consideration as an usual symmetric helicand thread. We have obtained a racemic mixture of (1*R*,2*R*)-*P* and (1*S*,2*S*)-*M* helices for Ni(*trans*-cyTs)·MeCN, whereas (1*R*,2*R*)-*M*, (1*S*,2*S*)-

M, (1*S*,2*S*)-*P* and (1*R*,2*R*)-*P* helices could be found for Cu(*trans*-cyTs)·MeCN.

Preliminary photophysical studies point to a relation between fluorescence and the presence of the tosylamino groups. The 1,2-diaminocyclohexane spacer avoids luminescence, whereas other spacers such as 1,2-diaminoethane or 1,3-diaminopropane do not prevent the fluorescence emission of their corresponding free ligands. Only the chelation of Zn(II) to $cyTs^{2-}$ involves an enhancement of the fluorescence emission.

Experimental

Materials and methods

Chemicals of the highest commercial grade available (Aldrich) were used as received. Iron, cobalt, nickel, copper, zinc and cadmium metals (Aldrich) were used as plates and washed with a dilute solution of hydrochloric acid prior to electrolysis.

Elemental analyses were performed on a Carlo Erba EA 1108 analyser. The NMR spectra were recorded on Bruker DPX-250 and DRX-500 spectrometers, using dmso-d_6 as solvent. Infrared spectra were recorded in the range of 4000–600 cm^{-1}, as KBr pellets on a Bio-Rad FTS 135 spectrophotometer. Mass spectra (FAB) were performed on a Micromass Autospec mass spectrometer, employing *m*-nitrobenzyl alcohol as matrix.

UV and fluorescence studies were carried out in 10^{-5} M acetonitrile solutions. Trifluoroacetic acid (TFA) was added (0–38 equivalents) to promote complex protonation. TFA was gradually added to the complex solution and the corresponding spectra were registered. The addition was interrupted when any change in absorption or emission spectra was observed. UV absorption spectra (200–400 nm) were recorded on a Perkin-Elmer Lambda 6 spectrophotometer and fluorescence emission spectra on a SPEX F111 Fluorolog spectrofluorimeter. Diffuse reflectance spectra were recorded on a Shimadzu UV-3103 PC spectrophotometer. UV-VIS spectra in DMF solution were registered on a HP 8452. A Varian E-109 spectrometer system was used to perform ESR measurements at 300 K.

X-Ray diffraction studies

The structure determinations were performed at room temperature on a Siemens CCD Diffractometer, using graphite-monochromated Mo-Kα radiation (λ = 0.71073 Å) from a fine focus sealed tube source. The structures were solved using Siemens SHELXTL-PC software[19] by direct methods and refined by full-matrix least-squares methods on F^2. All non-hydrogen atoms were anisotropically refined. All hydrogen atoms were included in the model at geometrically calculated positions and refined using a riding model. In the case of disordered atoms, their occupation sites were allowed to refine. Table 1 provides a summary of the crystal data, data collection and refinement parameters. Molecular graphics were represented by Ortep-3 for Windows[20] and RasWin.[21]

CCDC reference numbers 155428, 155429, 168560 and 168561.

See http://www.rsc.org/suppdata/dt/b1/b107116p/ for crystallographic data in CIF or other electronic format.

Ligand syntheses

H_2cyTs and (1*R*,2*R*)-H_2cyTs. *N*,*N*′-Bis(2-tosylaminobenzylidene)-1,2-diaminocyclohexane was prepared with an overall yield of 80%, following a three-step procedure (Scheme 1) as previously described.[5–7]

The first step involves the oxidation of **I** to give 2-aminobenzaldehyde (**II**).[22] Subsequently, the *N*-tosylation of **II** with tosyl chloride afforded **III**. Finally, a mixture of *cis*- and *trans*-1,2-diaminocyclohexane (0.204 g, 1.79 mmol) was added to a chloroform solution (150 cm^3) of **III** (1 g, 3.58 mmol). This mixture was heated (70 °C) and the volume of the solution was reduced to *ca.* 50 cm^3 over a 3 h period, using a Dean–Stark trap. The resultant yellow solution was filtered and then concentrated. The resultant powdery solid was collected by filtration, washed with diethyl ether (3 cm^3), and dried *in vacuo*. The (1*R*,2*R*)-(−)-isomer of the diamine was employed to prepare, with an identical procedure, the corresponding (1*R*,2*R*)-H_2cyTs ligand. Needle crystals of H_2cyTs and prismatic crystals of (1*R*,2*R*)-H_2cyTs·0.25H_2O, suitable for X-ray diffraction studies, were obtained by slow evaporation of saturated chloroform solutions of the corresponding powdery compounds. Yield 0.90 g (80%); mp 176 °C; dark-yellow solid. Found: C, 64.8; H, 5.8; N, 8.9; S, 10.1. Calc. for $C_{34}H_{36}N_4O_4S_2$: C, 64.9; H, 5.8; N, 8.9; S, 10.2%. IR spectroscopy (KBr, cm^{-1}): ν(N–H) 3431(w), ν(C=N) 1632(s), ν(C–N) 1335(s), $\nu_{as}(SO_2)$ 1289(s), $\nu_s(SO_2)$ 1157(s). FAB (*m*/*z*): 628.8 (100%, M^+). ^{1}H NMR (500 MHz, dmso-d_6, ppm): 13.22 (s, 2H, H_a), 8.62 (s, 2H, H_b), 7.41 (d, 4H, H_g), 7.36–7.31 (m, 6H, H_c, H_f, H_e), 7.01 (t, 2H, H_d), 6.66 (d, 4H, H_h), 3.53 (m, 2H, H_j), 1.99 (s, 6H, H_i), 1.96–1.86 (m, 4H, H_k), 1.71–1.52 (m, 4H, H_l). ^{13}C NMR data are deposited as ESI.† Fluorescence (MeCN, nm): 439(vw). UV (MeCN, nm): 222(vs), 260(s), 313(m).

(1*R*,2*R*)-H_2cy. *N*,*N*′-Bis(2-aminobenzylidene)-1,2-diaminocyclohexane was prepared by condensation of 2-aminobenzaldehyde (0.43 g, 3.58 mmol) with (1*R*,2*R*)-diaminocyclohexane (0.204 g, 1.79 mmol). Orange solid. Yield 0.47 g (83%). Found: C, 75.1; H, 7.6; N, 17.3. Calc. for $C_{20}H_{24}N_4$: C, 74.9; H, 7.5; N, 17.5%. FAB (*m*/*z*): 321.2 (100%, M^+); ^{1}H NMR (250 MHz, dmso-d_6, ppm): 8.25 (s, 2H, H_b), 7.11–7.07 (d, 2H, H_c), 7.00 (t, 2H, H_e), 6.60 (d, 2H, H_f), 6.45 (t, 2H, H_d), 3.21–3.17 (m, 2H, H_j), 1.82–1.80 (m, 4H, H_k), 1.66–1.39 (m, 4H, H_l); ^{13}C NMR data are deposited as ESI.† UV (MeCN, nm): 224(vs), 260(s), 343(m).

Complexes syntheses

Complexes have been obtained by an electrochemical method,[23] in which a metal anode was oxidized in an acetonitrile solution of H_2cyTs or (1*R*,2*R*)-H_2cy. A typical preparation is outlined below, *e.g.* Fe(cyTs)·2H_2O. The cell can be summarized as: $Fe_{(+)}|H_2cyTs + MeCN + NMe_4ClO_4|Pt_{(-)}$. An acetonitrile solution (80 cm^3) of H_2cyTs (100 mg, 0.159 mmol), containing about 10 mg of tetramethylammonium perchlorate, was electrolyzed for 1.7 h using a current intensity of 5 mA and a voltage of 9.3 V. A platinum wire was used as cathode and an iron sheet as anode. (**CAUTION:** Although no problem has been encountered in this work, all perchlorate compounds are potentially explosive, and should be handled in small quantities and with great care!) Filtration and concentration of the resulting solution to a third of its initial volume yielded a yellow solid that was washed with diethyl ether and vacuum dried.

We have isolated, with high purity and yield, the corresponding complexes M(cyTs)·$x$$H_2O$ (M = Fe, Co or Cu, x = 1–3), M(*trans*-cyTs)·$x$$H_2O$ (M = Ni, Zn or Cd, x = 1–3) and Zn(*trans*-cy)(MeCN). Prismatic crystals of Cu(*trans*-cyTs)·MeCN and Ni(*trans*-cyTs)·MeCN suitable for X-ray studies were obtained by slow evaporation of Cu(cyTs)·H_2O and Ni(*trans*-cyTs)·MeCN·3H_2O acetonitrile solutions, respectively.

Fe(cyTs)·2H_2O. Red solid. Yield 0.08 g (75%). Found: C, 56.6; H, 5.5; N, 7.9; S, 8.6. Calc. for $C_{34}H_{38}FeN_4O_6S_2$: C, 56.8; H, 5.3; N, 7.8; S, 8.9%. IR (KBr, cm^{-1}): ν(C=N) 1620(s), ν(C–N) 1288(s), $\nu_{as}(SO_2)$ 1260(s), $\nu_s(SO_2)$ 1133(s). FAB (*m*/*z*): 682,1 (2%, $M^+ - 2H_2O$). Magnetic moment: 5.1 μ_B. DR (nm): 1130 ($^5E_g \longleftarrow {}^5T_{2g}$).

Co(cyTs)·3H_2O. Dark red solid. Yield 0.09 g (80%). Found: C, 54.6; H, 5.5; N, 7.8; S, 8.1. Calc. for $C_{34}CoH_{40}N_4O_7S_2$: C, 55.1; H, 5.4; N, 7.6; S, 8.6%. IR (KBr, cm^{-1}): ν(C=N) 1634(s),

ν(C–N) 1285(s), $\nu_{as}(SO_2)$ 1266(s), $\nu_s(SO_2)$ 1128(s). FAB (*m*/*z*): 685.1 (37%, $M^+ - 3H_2O$). Magnetic moment: 4.5 μ_B. DR (nm): 1320 ($^4T_{2g} \longleftarrow {}^4T_{1g}$), 540 [$^4T_{1g}(P) \longleftarrow {}^4T_{21g}(F)$]. UV-VIS (DMF, nm): 545 [$^4T_{1g}(P) \longleftarrow {}^4T_{21g}(F)$].

Ni(*trans*-cyTs)·MeCN·3H$_2$O. Greenish brown solid. Yield 0.10 g (83%). Found: C, 55.8; H, 5.9; N, 8.8; S, 8.6. Calc. for $C_{36}H_{43}N_5NiO_7S_2$: C, 55.4; H, 5.5; N, 8.9; S, 8.2%. IR (KBr, cm^{-1}): ν(C=N) 1613(s), ν(C–N) 1289(s), $\nu_{as}(SO_2)$ 1262(s), $\nu_s(SO_2)$ 1138(s). FAB (*m*/*z*): 685.2 (19%, $M^+ - MeCN - 3H_2O$). ^{1}H NMR (250 MHz, dmso-d_6, ppm): 8.63 (s, 2H, H_b), 7.57 (d, 4H, H_g), 7.43–7.26 (m, 6H, H_c, H_f, H_e), 7.11 (d, 4H, H_h), 7.06 (t, 2H, H_d), 3.57–3.52 (m, 2H, H_j), 2.27 (s, 6H, H_i), 2.18–2.16 (m, 4H, H_k), 1.90–1.78 (m, 4H, H_l). DR (nm): 550 ($^1E_{1g} \longleftarrow {}^1A_{1g}$). UV-VIS (DMF, nm): 560 ($^1E_{1g} \longleftarrow {}^1A_{1g}$).

Cu(cyTs)·H$_2$O. Dark green solid. Yield 0.10 g (87%). Found: C, 57.2; H, 5.1; N, 7.9; S, 8.8. Calc. for $C_{34}CuH_{36}N_4O_5S_2$: C, 57.3; H, 5.0; N, 7.8; S, 9.0%. IR (KBr, cm^{-1}): ν(C=N) 1640(s), ν(C–N) 1281(s), $\nu_{as}(SO_2)$ 1257(s), $\nu_s(SO_2)$ 1134(s). FAB (*m*/*z*): 690.3 (100%, $M^+ - H_2O$). Magnetic moment: 2.0 μ_B. DR (nm): 560. UV-VIS (DMF, nm): 565. ESR (powder, 300 K, *g*): 2.05.

Zn(*trans*-cyTs)·3H$_2$O. Pale-yellow solid. Yield 0.09 g (75%). Found: C, 54.4; H, 5.0; N, 7.4; S, 8.8. Calc. for $C_{34}H_{40}N_4O_7S_2Zn$: C, 54.7; H, 5.3; N, 7.5; S, 8.6%. IR (KBr, cm^{-1}): ν(C=N) 1621(s), ν(C–N) 1293(s), $\nu_{as}(SO_2)$ 1262(s), $\nu_s(SO_2)$ 1138(s). FAB (*m*/*z*): 691.1 (100%, $M^+ - 3H_2O$). ^{1}H NMR (500 MHz, dmso-d_6, ppm): 8.61 (s, 2H, H_b), 7.72 (d, 4H, H_g), 7.63 (d, 2H, H_c), 7.30 (t, 2H, H_e), 7.25 (m, 6H, H_h, H_f), 6.98 (t, 2H, H_d), 3.59–3.57 (m, 2H, H_j), 2.33 (s, 6H, H_i), 1.95 (m. 4H, H_k), 1.55–1.45 (m, 4H, H_l). ^{13}C NMR data are deposited as ESI. † UV (MeCN, nm): 230(vs), 275(s), 346(m). Fluorescence (MeCN, nm): 435(s).

Cd(*trans*-cyTs)·2H$_2$O. Pale-yellow solid. Yield 0.10 g (81%). Found: C, 52.4; H, 4.7; N, 7.2; S, 8.3. Calc. for $C_{34}CdH_{38}N_4O_6S_2$: C, 52.6; H, 4.9; N, 7.2; S, 8.2%. IR (KBr, cm^{-1}): ν(C=N) 1617(s), ν(C–N) 1294(s), $\nu_{as}(SO_2)$ 1255(s), $\nu_s(SO_2)$ 1126(s). FAB (*m*/*z*): 740.1 (4%, $M^+ - 2H_2O$). UV (MeCN, nm): 223(vs), 260(s), 315(m), 362(vw). Fluorescence (MeCN, nm): 430(vw).

Zn(*trans*-cy)(MeCN). Pale-yellow solid. Yield 0.08 g (70%). Found: C, 62.0; H, 5.6; N, 16.7. Calc. for $C_{22}H_{27}N_5Zn$: C, 62.1; H, 5.8; N, 16.5%. FAB (*m*/*z*): 423.2 (8%, M^+). ^{1}H NMR (250 MHz, dmso-d_6, ppm): 8.30 (s, 2H, H_b), 7.47 (d, 2H, H_c), 7.24 (t, 2H, H_e), 7.11 (d, 2H, H_f), 7.02 (t, 2H, H_d), 3.90 (m, 2H, H_j), 1.91–1.55 (m, 8H, H_k, H_l). UV (MeCN, nm): 223(vs), 313(vw).

Acknowledgements

The authors thank Xunta de Galicia (PGIDT99XI20903B) for financial support. M.V. thanks Fundación Segundo Gil Dávila for a grant.

References

1 (*a*) M. J. Hannon, C. L. Painting, A. Jackson, J. Hamblim and W. Errington, *Chem. Commun.*, 1997, 1807; (*b*) M. J. Hannon, S. Bunce, A. J. Clarke and N. W. Alcock, *Angew. Chem., Int. Ed.*, 1998, **38**, 1277; (*c*) M. J. Hannon, C. L. Painting and N. W. Alcock, *Chem. Commun.*, 1999, 2023.
2 (*a*) J. Sanmartín, M. R. Bermejo, A. M. García-Deibe and A. Llamas, *Chem. Commun.*, 2000, 795; (*b*) J. Sanmartín, M. R. Bermejo, A. M. García-Deibe, I. M. Rivas and A. R. Fernández, *J. Chem. Soc., Dalton Trans.*, 2000, 4174.
3 J. Sanmartín, M. R. Bermejo, A. M. García-Deibe, O. Piro and E. E. Castellano, *Chem. Commun.*, 1999, 1953.
4 (*a*) M. Vázquez, M. R. Bermejo, M. Fondo, A. M. González, J. Mahía, L. Sorace and D. Gatteschi, *Eur. J. Inorg. Chem.*, 2001, 1863; (*b*) M. Vázquez, M. R. Bermejo, M. Fondo, A. García-Deibe, A. M. González and R. Pedrido, *Eur. J. Inorg. Chem.*, 2002, 465–472.
5 (*a*) J. Mahía, M. Maestro, M. Vázquez, M. R. Bermejo, J. Sanmartín and M. Maneiro, *Acta Crystallogr., Sect. C*, 1999, **55**, 1545; (*b*) J. Mahía, M. Maestro, M. Vázquez, M. R. Bermejo, A. M. González and M. Maneiro, *Acta Crystallogr., Sect. C*, 2000, **56**, 347; (*c*) J. Mahía, M. Maestro, M. Vázquez, M. R. Bermejo, A. M. González and M. Maneiro, *Acta Crystallogr., Sect. C*, 2000, **56**, 492.
6 L. Prodi, F. Bolletta, M. Montalti and N. Zaccheroni, *Eur. J. Inorg. Chem.*, 1999, 455.
7 L. Prodi, F. Bolletta, M. Montalti and N. Zaccheroni, *Coord. Chem. Rev.*, 2000, **205**, 59.
8 H. E. Gottlieb, V. Kotlyar and A. Nudelman, *J. Org. Chem.*, 1997, **62**, 7512.
9 E. H. Charles, L. M. L. Chia, J. Rothery, E. L. Watson, E. J. L. McInnes, R. D. Farley, A. J. Bridgeman, F. E. Mabbs, C. C. Rowlands and M. A. Halcrow, *J. Chem. Soc., Dalton Trans.*, 1999, 2087.
10 (*a*) G. C. Van Stein, G. Van Koten, K. Vrieze, C. Brevard and A. L. Spek, *J. Am. Chem. Soc.*, 1984, **106**, 4486; (*b*) G. C. Van Stein, G. Van Koten, H. Passenier, O. Steinebach and K. Vrieze, *Inorg. Chim. Acta*, 1984, **89**, 79; (*c*) G. C. Van Stein, H. Van der Poel, G. Van Koten, A. L. Spek, A. J. M. Duisenberg and P. S. Pregosin, *J. Chem. Soc., Chem. Commun.*, 1980, 1016; (*d*) G. C. Van Stein, G. Van Koten, F. Blank, L. C. Taylor, K. Vrieze, A. L. Spek, A. J. M. Duisenberg, A. M. M. Schreurs, B. Kojic-Prodic and C. Brevard, *Inorg. Chim. Acta*, 1985, **98**, 107.
11 J. Mahía, M. Maestro, M. Vázquez, M. R. Bermejo, A. M. González and M. Maneiro, *Acta Crystallogr., Sect. C*, 1999, **55**, 2158.
12 M. R. Bermejo, A. Sousa, M. Fondo and M. Helliwell, *New. J. Chem.*, 2000, **24**, 33.
13 L. Gutierrez, G. Alzuet, J. A. Real, J. Cano, J. Borras and A. Castiñeiras, *Inorg. Chem.*, 2000, **39**, 3608.
14 A. Sousa, M. R. Bermejo, M. Fondo, A. García-Deibe, A. Sousa-Pedrares and O. Piro, *New. J. Chem.*, 2001, **25**, 647.
15 R. D. Shannon, *Acta Crystallogr., Sect. A*, 1976, **32**, 751.
16 (*a*) C. Piguet, G. Bernardinelli and G. Hopfgartner, *Chem. Rev.*, 1997, **97**, 2006; (*b*) C. Piguet and J.-C. G. Bünzli, *Chem. Soc. Rev.*, 1999, **28**, 347; (*c*) F. Renaud, C. Piguet, G. Bernardinelli, J.-C. G. Bünzli and G. Hopfgartner, *J. Am. Chem. Soc.*, 1999, **121**, 9326.
17 (*a*) E. C. Constable, *Prog. Inorg. Chem.*, 1994, **42**, 67; (*b*) E. C. Constable, *Comprehensive Supramolecular Chemistry*, ed. J. L. Atwood, J. E. D. Davies, D. D. MacNikol, F. Vögtle, and K. S. Suslick, Pergamon, Oxford, 1996, vol. 9, p. 213.
18 See for example (*a*) E. C. Constable, T. Kulke, M. Neuburger and M. Zehnder, *Chem. Commun.*, 1997, 489; (*b*) E. C. Constable, T. Kulke, G. Baum and D. Fenske, *Inorg. Chem. Commun.*, 1998, **1**, 80; (*c*) J. M. Lehn, *Supramolecular Chemistry-Concepts and Perspectives*, VCH, Weinheim, 1995; (*d*) J.-M. Lehn and P. Ball, *New Chem.*, 2000, 300; (*e*) A. von Zelwsky and O. Mamula, *J. Chem. Soc., Dalton Trans.*, 2000, 219 and references therein.
19 G. M. Sheldrick, SHELX-97 (SHELXS 97 and SHELXL 97), Programs for Crystal Structure Analyses, University of Gottingen, Germany, 1998.
20 L. J. Farrugia, *J. Appl. Crystallogr.*, 1997, **30**, 565.
21 R. Sayle, RasWin Molecular Graphics Windows version 2.6-ucb, Glaxo Research and Development, Greenford, Middlesex, UK, 1995.
22 W. K. Anderson and D. K. Dalvie, *J. Heterocycl. Chem*, 1993, **30**, 1533.
23 M. R. Bermejo, A. M. González, M. Fondo, A. García-Deibe, M. Maneiro, J. Sanmartín, O. L. Hoyos and M. Watkinson, *New. J. Chem.*, 2000, **24**, 235.